Influence of Ionic Coordination on the Cathode Reaction Mechanisms of Al/S Batteries

Bhowmik, Arghya; Carrasco-Busturia, David; Jankowski, Piotr; Raccichini, Rinaldo; Garcia-Araez, Nuria; García-Lastra, Juan María

Published in:
Journal of Physical Chemistry C

Link to article, DOI:
10.1021/acs.jpcc.1c08426

Publication date:
2022

Document Version
Peer reviewed version

Influence of the ionic coordination on the cathode reaction mechanisms of Al/S batteries

Arghya Bhowmik*[1], David Carrasco-Busturia[1], Piotr Jankowski[1], Rinaldo Raccichini[2], Nuria Garcia-Araez[2], Juan María García-Lastra*[1]

[1]Department of Energy Conversion and Storage, Technical University of Denmark, 2800 Kgs. Lyngby, Denmark

[2]Department of Chemistry, University of Southampton, University Road, Southampton SO17 1BJ United Kingdom

* email: arbh@dtu.dk (Bhowmik) and jmgla@dtu.dk (García-Lastra)

Abstract

Lack of knowledge on electrochemical reaction pathways for Al/S batteries prevents the development of practical approaches to mitigate the irreversibility and poor cycling performances of this appealing secondary battery system which is, in theory, scalable, inexpensive, and energy-dense. Different from the Li/S system, Al/S batteries use ionic liquids (ILs) as electrolytes. The choice of the IL, i.e., whether the IL is based on a conventional EMImCl-based electrolyte or in a deep eutectic mixture of aluminum chloride with Urea (or any of its derivatives), strongly affects the electrochemical energy storage performances of the cell. To shed some light on the Al/S battery chemistry, here, we present a computational electrochemistry research work to determine the most favorable reaction pathways and thermodynamically stable reaction intermediates. We also discuss the effect of the coordination of ionic species (originated from aluminum-containing deep eutectic electrolytes) with polysulfide intermediates which lead to alterations in the reaction pathway and electrochemical behavior of the Al/S system. The spectroscopic signatures from various reaction intermediates are also reported and validated via comparison with experimental observations.

1. Introduction

Carbon neutral electricity supply needs grid-scale energy storage[1] to balance the fluctuating renewable resources. While pumped hydro storage provides the lowest life cycle cost, it can not be deployed everywhere on a mass scale due to geography and environmental impact limitations. Rechargeable batteries are critical in energy grids' reliability and utilization when the generative capacity of the grid is primarily renewables. Innovating beyond the state-of-the-art lithium-ion batteries is crucial for the battery research community to generate cost-effective electrochemical energy storage solutions for the grid. For example, coupling an aluminum anode with a sulfur cathode could produce low-cost, safe, high-energy-density rechargeable Al/S cells. Combining a three-electron per aluminum anode reaction and a two-electron per atomic sulfur cathode reaction makes a battery with theoretical specific energy close to 1300 Wh kg^{-1} [2–4]. In addition, aluminum and sulfur are both cheap, easy to produce, earth-abundant materials. Thus such battery chemistry is, in principle, scalable to TWhs - a requirement for grid deployment across the world. The electrochemical behavior of sulfur-based cathode in non-aqueous, aluminum-based systems was investigated for the first time in NaCl-$AlCl_3$ electrolytes melt in 1984[5], in pyridinium ionic liquid in 1985[6], and aqueous alkaline electrolytes for the same were reported as early as 1993[7]. However, the progress has been slow, with relatively few articles published on Al/S chemistry until recently. The discovery of an ionic liquid-based Al/S battery a few years ago[8] opened a new direction in this battery chemistry, and more research results have been published last few years than all the previous years combined[9–18]. In addition, significant recent work have focused on aluminum ion batteries[19–23].

The interest in Al/S batteries rose particularly after a new group of urea/acetamide and $AlCl_3$ based deep eutectic solvent (DES) electrolytes were recently proposed for the Al/S battery system[9,10,16]. Unlike the conventional ionic liquids, like, for example, those based on the organic 1-Ethyl-3-methylimidazolium chloride (EMImCl), these "new" electrolytes made of cost-effective components are inexpensive to produce as the synthesis is straightforward. Additionally, in Al/S batteries, these DES electrolytes enable the delivery of higher capacity than EMImCl-based electrolyte[10], thus raising the question of whether the reaction mechanism is altered when the DES electrolytes are used.

The operation of Al/S batteries involves the oxidation of the aluminum at the negative electrode and the reduction of the sulfur at the positive electrode during the discharge process and vice versa for the recharge process. Unfortunately, the reaction mechanisms are poorly understood, thus, limiting further progress towards the circumvention or overcome of the current Al/S battery system limitations such as low discharge potential, sluggish reaction kinetics, large voltage hysteresis (low round trip efficiency), and limited cycle life. Experimental studies on ionic liquid-based Al/S cells show single discharge and charge plateaus. This behavior is quite distinctive from the typical two-stage voltage profile in Li/S system[24,25] Based on electrochemical and spectroscopic data, it has been proposed that the reaction mechanism in Al/S batteries goes through the formation of a series of polysulfides, with Al_2S_3 as the final discharge product, in analogy to the Li/S system[14,15,24,25]. However, the details of the reaction mechanisms remain unclear, and the interaction between polysulfides and sulfide with aluminum ions is expected to be much stronger and complex than with lithium ions. Furthermore, the role of the chemical composition of the electrolyte on the reaction mechanism also remains largely unexplored.

Recent ab-initio molecular dynamics simulations have demonstrated that the reactivity, speciation, and transport properties of DES electrolytes depend on a complex balance of different types of complex interactions[11,26]. Therefore, investigating the interaction of aluminum ions with polysulfides and ionic species in the electrolyte is paramount to understanding the reaction mechanisms in Al/S batteries' cathodes. For example, by roughly considering the theory of electrolytic conductance[27], it is highly unlikely to find triple-charge Al^{3+} ions not coordinated with the ionic species present in the electrolyte. A previous theoretical study of the Al/S system, also using ab-initio molecular dynamics simulations, attempted to elucidate the reaction mechanism, but unfortunately, the critical role of the coordination of aluminum ions with electrolyte species was overlooked[12].

In this work, we employ ab-initio calculations to elucidate the most likely species involved in Al/S battery reactions and provide new findings on the reaction mechanisms. In our research work, we consider both EMImCl-based and DES (particularly the Urea-based system) electrolytes. We demonstrate that Al atoms prefer four-fold coordination. Consequently, the mechanism of Al/S battery reactions involves a series of steps in which Al/S bonds sequentially replace some of the Al-Cl bonds present in the initial electrolyte species (e.g., $AlCl_4^-$, $Al_2Cl_7^-$). Based on the available data and the results of the calculations, we propose the most likely pathways for Al/S battery reactions.

Simulation details are provided in section 2 followed by description and stability of reaction intermediates in section 3.1. Section 3.2 contain thermodynamics analysis of reaction networks with and without the participation of IL species. In section 3.3, we review experimentally observed charge discharge curve and spectroscopic characterizations to ascertain the validity of our theoretical work towards elucidation of the reaction mechanism.

2. Computational details

2.1. Methods and parameters

All simulations were carried out with the Amsterdam Density Functional suite (ADF) 2017 version[28]. Molecular structures were optimized with a triple-ζ double-polarized (TZ2P) basis set and B3LYP[29] functional and dispersion correction by Grimme[30] following simulations done for Li/S system[31]. Implicit solvation model COSMO[32] with a dielectric constant of 15 was used following reported values for ILs[33]. Free energy at 400K was estimated using calculated vibrational modes considering zero-point energy, vibrational enthalpy, and entropy contributions. IR and UV-vis spectra calculations were calculated with B3LYP functional, but Raman spectra calculations were done with RPBE due to limitations in implementation in ADF. Free energies of Solid state phases Al and Al_2S_3 were calibrated using known energetics[34,35] as ADF is built for non-periodic systems, but the results discussed in this article do not depend on the variations on these solid phase energies.

Reactions at the electrode-electrolyte interface of batteries are analogous to those in electro-catalysis, where the potential dependence of elementary reactions is often accessed via density functional theory-based simulations along with the “computational hydrogen electrode” concept[36]. The original version of the model relates the chemical potential of a proton/electron pair, at 0 V-RHE, to that of H_2 gas through the reference electrode reaction. Following this, an analogous computational aluminum reference electrode can be defined via the following reaction:

$$Al + 7AlCl_4^- = 4Al_2Cl_7^- + 3e^- \quad (1)$$

However, in the case of Urea/$AlCl_3$ electrolytes, the predominant electrolyte species are aluminum ions coordinated with chloride and urea ligands, such as $AlCl_2Urea^+$ and $4AlCl_2Urea_2^+$, and $AlCl_4^-$ [11,37]. Therefore, the following reaction is more appropriate as a reference:

$$Al + AlCl_2(Urea)_2^+ + 6AlCl_4^- = Al_2Cl_5(Urea)_2^+ + 3Al_2Cl_7^- + 3e^- \quad (2)$$

We employ the reactions above to report the potentials of the different reactions against the aluminum reference electrode potential scale.

The calculation of the potential-dependent Gibbs energies of reduction reactions is done as follows:

$$\Delta G^\circ = \Delta G^\circ(E=0\ V) + n\,E \quad (3)$$

where ΔG° is the Gibbs energy of the reaction at a potential E, $\Delta G^\circ(E=0\ V)$ is the Gibbs energy of the reaction at a potential equal to zero (against the reference, see reactions (1) and (2)), and n is the number of electrons involved in the reduction reaction.

3. Results and discussion

3.1. Reaction intermediates: structural and spectroscopic fingerprints

Sulfur is a molecular solid with weakly bound S_8 clusters forming a crown structure at standard conditions. Thus, our reaction tree search starts from a crown-shaped S_8 cluster following similar work done for Li/S battery[38]. We explored an extensive network of possible reactions, including reaction intermediates that are pure polysulfides (with various possible chain lengths, S_x^{2-}) and those that are coordinated with aluminum ions. We also took into account that Al^{3+} ions are not "free" but coordinated with chlorine to form $AlCl_4^-$ or $Al_2Cl_7^-$. When deep eutectics are used, aluminum ions are also coordinated by the neutral deep eutectic components (e.g., Urea)[9,11,26,37]. Consequently, we considered that reaction intermediates can consist of ions made of Al/Cl/S_x and deep eutectic components like Urea. For the polysulfides involved in the reactions, we considered all possible polysulfide chain lengths from sulfide (S^{2-}) to the eight-member polysulfide anion S_8^{2-}, hence the possible intermediates varied as S^{2-}_x(x=1,2,3,4,5,6,7,8).

3.1.1. Reaction intermediates in conventional ionic liquids

Conventional ionic liquid electrolytes used for Al/S batteries[8,10,15,24,25] are prepared by mixing an organic salt like EMImCl with $AlCl_3$ in excess, thus producing $AlCl_4^-$ and $Al_2Cl_7^-$. Under those conditions, the discharge of the battery will induce the reduction of sulfur to polysulfides:

$$x/8\ S_8 + 2e^- = S_x^{2-} \quad (4)$$

However, the formed polysulfides are unlikely to be uncoordinated. Instead, the polysulfide will coordinate aluminium ions, by replacing one or more of the chloride ligands in the $AlCl_4^-$ and $Al_2Cl_7^-$ complexes as follows:

$$S_x^{2-} + AlCl_4^- = AlCl_3S_x^{2-} + Cl^- \quad (5)$$
$$AlCl_3S_x^{2-} = AlCl_2S_x^- + Cl^- \quad (6)$$
$$S_x^{2-} + AlCl_4^- = AlCl_2S_x^- + 2Cl^- \quad (7)$$
$$S_x^{2-} + Al_2Cl_7^- = AlCl_4^- + AlCl_3S_x^{2-} \quad (8)$$

Consequently, we propose that the most likely reaction intermediates are aluminum-coordinated polysulfides of the type $AlCl_3S_x^{2-}$ and $AlCl_2S_x^-$. We elucidate the most stable structures of all these possible reaction intermediates through ab-initio calculations, and we show the results in Figure 1.

To evaluate the relative stability of the various polysulfide intermediates, we took into account that the Cl^- formed in the reactions of substitution of chloride ligand by polysulfides around the coordination sphere of aluminum ions (reactions 5-8) will likely react with $Al_2Cl_7^-$ to form $AlCl_4^-$ as follows:

$$Al_2Cl_7^- + Cl^- = 2AlCl_4^- \quad (9)$$

Consequently, the overall reaction of formation of $AlCl_3S_x^{2-}$ and $AlCl_2S_x^-$ intermediates can be written as:

$$S_x^{2-} + 2Al_2Cl_7^- = AlCl_2S_x^- + 3AlCl_4^- \quad (10)$$
$$S_x^{2-} + Al_2Cl_7^- = AlCl_3S_x^{2-} + AlCl_4^- \quad (11)$$
$$AlCl_3S_x^{2-} + Al_2Cl_7^- = AlCl_2S_x^- + 2AlCl_4^- \quad (12)$$

With the knowledge of the energies of all the possible reaction intermediates obtained from the DFT calculations, we obtained a quantitative estimation of the relative stability of all the possible intermediates, which we define as the Gibbs energies of reactions 10,11, and 12. The results are summarized in Table 1.

The Gibbs energies of reactions 10 and 11 are all negative, regardless of the polysulfide chain length, thus confirming the initial hypothesis that polysulfides will not be present as uncoordinated species in Al/S batteries. This is because the strength of the bond between polysulfides and aluminum cations is stronger than between chloride anions and aluminum cations. Hence, the ligand exchange reactions in which polysulfides displace chloride anions coordinating aluminum are thermodynamically favorable.
On the other hand, the fact that the energies of reaction 12 are also negative, regardless of the polysulfide chain length, demonstrate that polysulfides are more prone to bind as bidentate ligands rather than monodentate ligands.

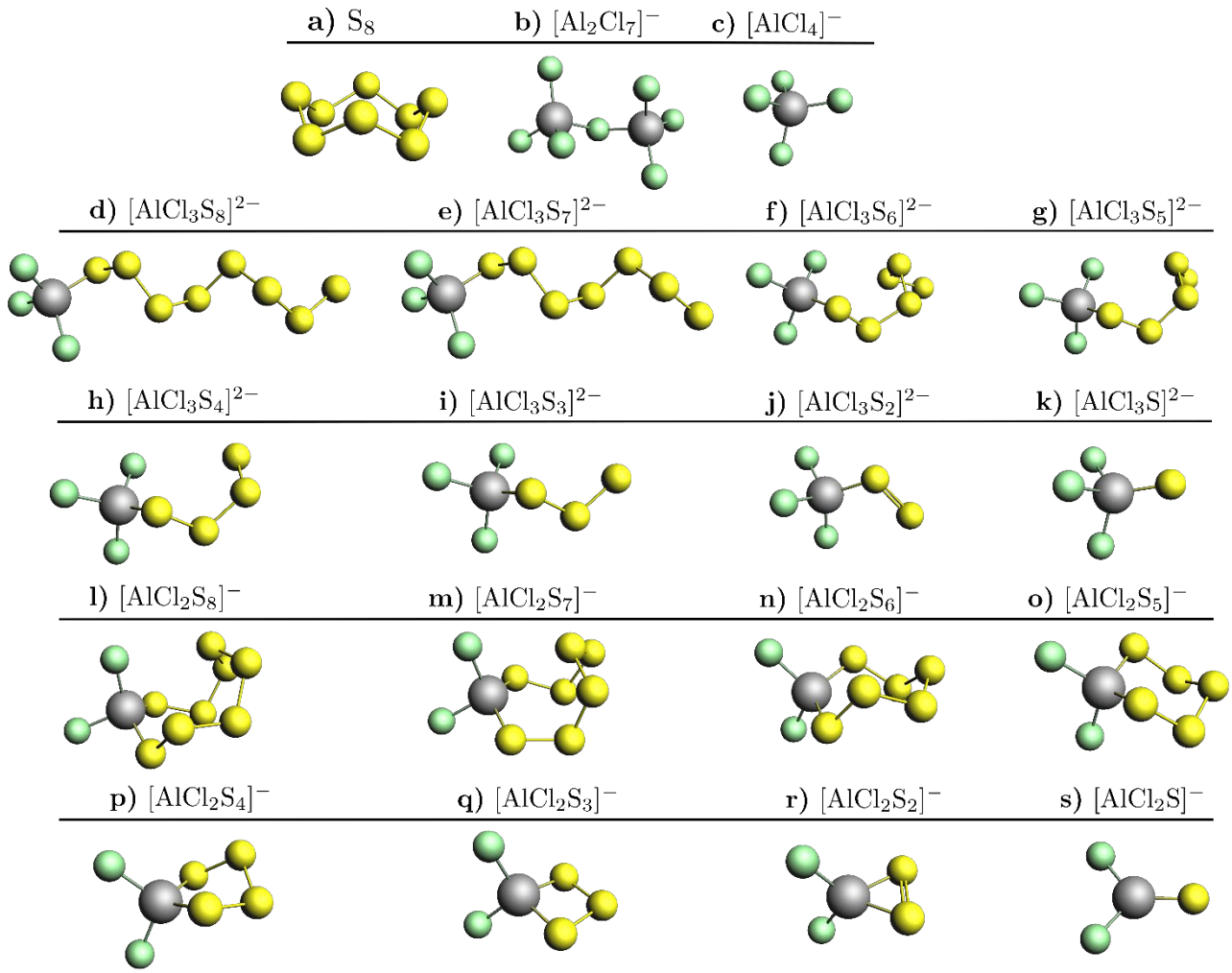

Figure 1: Optimized geometries of the various reaction intermediates in Al/S batteries in conventional (e.g. EMImCl-based) electrolytes, drawn in ball/stick form, for (a)S_8 (b)$Al_2Cl_7^-$ (c) $AlCl_4^-$ (d-k) $AlCl_3S_x^{2-}$ and (l-s) $AlCl_2S_x^-$ for x=1 to 8. Grey, yellow and green balls represent Al, S and Cl atoms, respectively.

Table 1: Gibbs free energy change of reactions 10 and 11 as predictors of the thermodynamic stability of intermediate compounds in Al/S batteries reactions (consisting of aluminum coordinated by chloride and polysulfide anions, $AlCl_3S_x^{2-}$ and $AlCl_2S_x^-$) with respect to uncoordinated polysulfides (S_x^{2-}), as a function of the number of sulfur atoms in the polysulfide chain length. The Gibbs energy of reaction 12, involving the transformation of polysulfide ligands from monodentate to bidentate to aluminum ions, is also included. All calculations are carried out at 400 K.

Polysulfide chain length (i.e. x in S_x^{2-})	8	7	6	5	4	3	2	1
Thermodynamic stability of $AlCl_3S_x^{2-}$ w.r.t S_x^{2-} (eV) via reaction 10	-3.70	-1.26	-1.16	-1.13	-1.15	-1.42	-1.58	-2.81
Thermodynamic stability of $AlCl_2S_x^-$ w.r.t S_x^{2-} (eV) via reaction 11	-5.28	-2.62	-2.89	-2.83	-2.79	-2.66	-2.89	-3.51
Thermodynamic stability of $AlCl_2S_x^-$ w.r.t $AlCl_3S_x^{2-}$ (eV) via reaction 12	-1.58	-1.36	-1.73	-1.70	-1.63	-1.24	-1.31	-0.70

3.1.2. Reaction intermediates in deep eutectic electrolytes

Deep eutectic electrolytes prepared by mixing $AlCl_3$ and Urea contain a complex mixture of species made of aluminum ions coordinated with chloride anions and Urea like $AlCl_2(Urea)_2^+$, in addition to the $AlCl_4^-$ anions[11,37]. Thus, reaction intermediates in the reduction pathway of S_8 to Al_2S_3 will contain aluminum ions coordinated to a mixture of ligands, including chlorine, Urea, and polysulfides. As mentioned above, the reduction of sulfur produces polysulfides (reaction 1), which will be eager to induce ligand exchange reactions to coordinate aluminum ions:

$S_x^{2-} + AlCl_2(Urea)_2^+ = AlCl_2S_x^- + 2Urea$ (13)
$S_x^{2-} + AlCl_2(Urea)_2^+ = AlCl_2(Urea)S_x^- + Urea$ (14)
$S_x^{2-} + AlCl_2(Urea)_2^+ = AlCl(Urea)S_x + Urea + Cl^-$ (15)
$S_x^{2-} + AlCl_4^- = AlCl_3S_x^{2-} + Cl^-$ (16)
(Reaction 16 is identical to reaction 5, but it is included here for completeness)

And some of the products of the above reactions (Cl^- and Urea) will then react further as follow:

$2\ Urea + Al_2Cl_7^- + Al_2Cl_5(Urea)_2^+ = 2\ AlCl_4^- + 2\ AlCl_2(Urea)_2^+$ (17)
$Cl^- + Al_2Cl_5(Urea)^+ = AlCl_2(Urea)_2^+ + AlCl_4^-$ (18)

Combining the reactions 13-16 with reactions 17-18 give the following overall reactions of coordination of polysulfides with aluminum ions via reactions that involve the predominant species[39] present in the urea-based eutectic electrolytes:

$S_x^{2-} + Al_2Cl_5(Urea)_2^+ + Al_2Cl_7^- = AlCl_2S_x^- + AlCl_2(Urea)_2^+ + 2AlCl_4^-$ (19)
$S_x^{2-} + ½\ Al_2Cl_5(Urea)_2^+ + ½\ Al_2Cl_7^- = AlCl_2(Urea)S_x^- + AlCl_4^-$ (20)
$S_x^{--} + ½\ Al_2Cl_5(Urea)_2^+ + 3/2\ Al_2Cl_7^- = AlCl(Urea)S_x + 3AlCl_4^-$ (21)
$S_x^{--} + Al_2Cl_5(Urea)_2^+ = AlCl_3S_x^{2-} + AlCl_2(Urea)_2^+$ (22)

By computing the Gibbs energy of the reactions 19 to 22, we quantitatively evaluate the possibility of the polysulfide species formed in urea-based eutectic electrolytes to remain uncoordinated or bond with aluminum ions. The optimized structures of the possible reaction intermediates are shown in Figure 2, and the results of the computation of the Gibbs energy of the reactions are disclosed in Table 2. In all cases, the values of the Gibbs energies of the reactions are negative, thus confirming that uncoordinated polysulfides are not stable in the eutectic electrolyte, as similarly reported in the case of “conventional” (i.e., EMImCl-based) electrolyte.

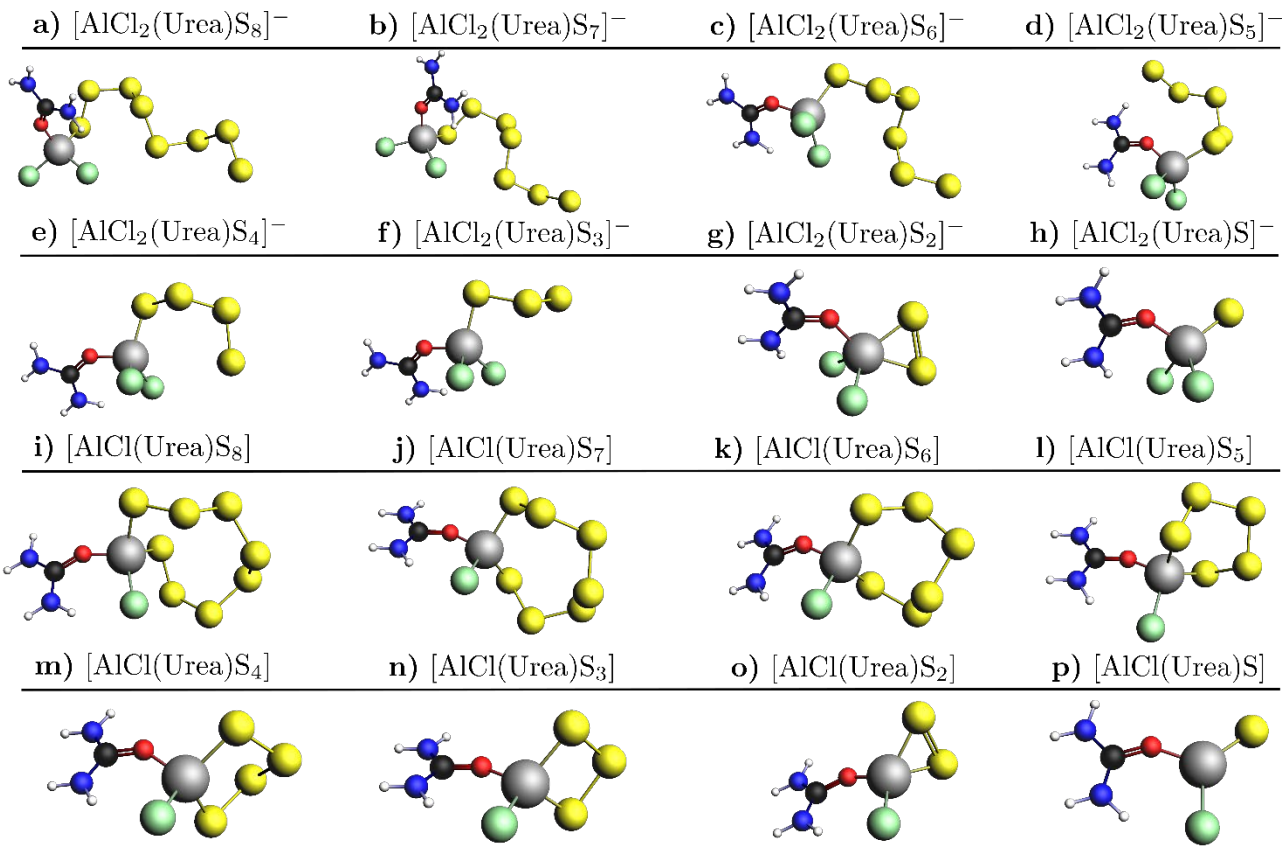

Figure 2: As in Figure 1 but for the intermediates in Al/S batteries with urea-based deep eutectic electrolytes, for (a-h) $AlCl_2(Urea)S_x^-$ and (i-p) $AlCl(Urea)S_x$ for x=1 to 8. Grey, yellow, green, red, blue, black and white balls represent Al, S, Cl, O, N, C, and H atoms, respectively.

Table 2: Gibbs free energy change of reactions 19 to 22 as predictors of the thermodynamic stability of intermediate compounds in Al/S batteries reactions (consisting of aluminum coordinated by chloride, urea and polysulfide anions, such as $AlCl_2S_x^-$, $AlCl_2(Urea)S_x^-$, $AlCl(Urea)S_x$ and $AlCl_3S_x^{2-}$) with respect to uncoordinated polysulfides (S_x^{2-}), as a function of the number of sulfur atoms in the polysulfide chain length. All calculations are carried out at 400 K.

Polysulfide chain length (i.e. x in S_x^{2-})	8	7	6	5	4	3	2	1
Thermodynamic stability of $AlCl_2S_x^-$ w.r.t S_x^{2-} (eV) via reaction 19	-5.36	-2.70	-2.97	-2.91	-2.87	-2.74	-2.97	-3.60
Stability of $AlCl_2(Urea)S_x^-$ w.r.t S_x^{2-} (eV) via reaction 20	-4.31	-2.14	-1.92	-1.65	-1.39	-1.72	-2.11	-3.19
Stability of $AlCl(Urea)S_x$ w.r.t S_x^{2-} (eV) via reaction 21	-5.81	-3.50	-3.24	-3.39	-3.38	-3.30	-3.52	-4.66
Stability of $AlCl_3S_x^{2-}$ w.r.t S_x^{2-} (eV) via reaction 22	-4.80	-2.36	-2.26	-2.23	-2.26	-2.52	-2.69	-3.91

We estimate that double coordination to the polysulphide chain is energetically preferred over coordination to additional Cl atoms (Table 2). The trend remains similar for intermediates where Al does not have any Urea coordination (Table 1). For both $AlCl_2S_x^-$ and $AlCl(Urea)S_x$, the Al atom is doubly coordinated with the polysulfide chain.
We would also like to point out that the $AlCl_3S_x^{2-}$ and $AlCl_2S_x^-$ intermediates are more likely to be formed from the IL cations' reaction for DES electrolytes. However, $AlCl_2S_x^-$ are the most likely intermediates irrespective of the type of electrolyte. $AlCl(Urea)S_x$ are also likely intermediates for Urea/$AlCl_3$ based IL.

3.2. Reaction paths: participation of electrolyte species

The analysis carried out in the previous section provides free energy correlations between possible intermediates that significantly reduce the reaction network region, which need to be explored to find the correct pathway toward the Al_2S_3 formation. Firstly, we can consider $AlCl_2S_x^-$ as the primary reaction intermediate, and then the reaction pathway in the deep eutectic solvent electrolytes is studied by incorporating the presence of $AlCl(Urea)S_x$ species. The polysulfide redox reactions are consider to consist of two-electron ractions that produce the cleavage of a sulfur-sulfur bond in the polysulfide sulfur chain. The reaction steps that are most likely to be part of the actual reaction network are highlighted in bold in the following sections.

3.2.1. Reaction network without IL participation

In absence of complex cations like $AlCl_2(Urea)S_x^-$ and $AlCl(Urea)S_x$, the Al electrode redox reactions involves $AlCl_4^-$ and $Al_2Cl_7^-$ species, which we use as the reference electrode reaction, see reaction (1). In the following, values of potentials of the different reactions, given against that reference, are denoted with the label (A), and the most likely (i.e. most favorable) steps involved in the discharge reaction of the sulfur electrode are highlighted in bold. The sulfur electrode reactions start with the opening of the S_8 molecule chain via a two-electron reduction reaction:

$S_8 + 2Al_2Cl_7^- + 2e^- = AlCl_2S_8^- + 3AlCl_4^-$ **1.28 V** *vs.* (A) (23)

The reaction is downhill in energy by 2.56 eV in this reference electrode scale. Following reaction steps where $AlCl_2S_8^-$ polysulfide chain further breaks can lead to both symmetrical breaking to $AlCl_2S_4^-$ or production of asymmetrical species generated by the combination of $AlCl_2S_7^- + AlCl_2S^-$, $AlCl_2S_6^- + AlCl_2S_2^-$, $AlCl_2S_5^- + AlCl_2S_3^-$. Our calculations show that symmetrical breaking is preferred over asymmetrical chain breaking. The S-S bond-breaking is easier to happen in an S-S bond that is further off from the Al-S bond.

$AlCl_2S_8^- + 2Al_2Cl_7^- + 2e^- = AlCl_2S_7^- + AlCl_2S^- + 3AlCl_4^-$ 0.95 V *vs.* (A) (24)
$AlCl_2S_8^- + 2Al_2Cl_7^- + 2e^- = AlCl_2S_6^- + AlCl_2S_2^- + 3AlCl_4^-$ 1.21 V *vs.* (A) (25)
$AlCl_2S_8^- + 2Al_2Cl_7^- + 2e^- = AlCl_2S_5^- + AlCl_2S_3^- + 3AlCl_4^-$ 1.31 V *vs.* (A) (26)
$AlCl_2S_8^- + 2Al_2Cl_7^- + 2e^- = 2AlCl_2S_4^- + 3AlCl_4^-$ **1.43 V** *vs.* (A) (27)

The $AlCl_2S_4^-$ formed is further oxidised into $AlCl_2S_2^-$ or $AlCl_2S_3^- + AlCl_2S^-$ with transfer of two additional electrons.

$AlCl_2S_4^- + 2Al_2Cl_7^- + 2e^- = AlCl_2S_3^- + AlCl_2S^- + 3AlCl_4^-$ **0.88 V** *vs.* (A) (28)
$AlCl_2S_4^- + 2Al_2Cl_7^- + 2e^- = 2AlCl_2S_2^- + 3AlCl_4^-$ **0.83 V** *vs.* (A) (29)

The formation of $AlCl_2S_3^-$ is thermodynamically favored, and $AlCl_2S_2^-$ is also expected to be produced. Further splitting of S-S bonds in these intermediates leads to the smallest species in the $AlCl_2S_x^-$ series.

This thermodynamically degenerated step reaction for the smaller polysulfides helps create a 1:1 ratio of $AlCl_2S_2^-$: $AlCl_2S^-$ species needed for Al_2S_3 formation.

$AlCl_2S_3^- + 2Al_2Cl_7^- + 2e^- = AlCl_2S_2^- + AlCl_2S^- + 3AlCl_4^-$ **0.94 V** vs. (A) (30)

$AlCl_2S_2^- + 2Al_2Cl_7^- + 2e^- = 2AlCl_2S^- + 3AlCl_4^-$ **0.99 V** vs. (A) (31)

Finally, Al_2S_3 is formed:

$AlCl_2S_2^- + AlCl_2S^- + 4Al_2Cl_7^- + 2e^- = Al_2S_3 + 8AlCl_4^-$ **0.96 V** vs. (A) (32)

The discharge potentials of the reactions identified as the most likely steps of the overall discharge reaction mechanism (23, 27, 28/29, 30/31, 32) are 1.28, 1.43, 0.83/0.88, 0.94/0.99, 0.96 V respectively, given against the Al electrode reference scale. As the observable potential is limited by the smallest discharge potential leading to it, we foresee the main discharge plateau at 0.83 V at a low discharge rate (i.e., in the absence of kinetic overpotentials). On the other hand, the charging plateau is controlled by the largest step. Thus the main charging plateau is expected at 1.43 V.

3.2.2. Reaction network when IL participates

In the presence of complex cations like $AlCl_2(Urea)S_x^-$ and $AlCl(Urea)S_x$, the Al electrode redox reactions proceed via reaction (2). In the following, values of potentials of different reactions given against this reference are denoted with the label (B), and the most likely (i.e. most favorable) steps are highlighted in bold. The sulfur electrode reactions start with the opening of the S_8 chain:

$S_8 + Al_2Cl_5(Urea)_2^+ + Al_2Cl_7^- + 2e^- = AlCl_2S_8^- + AlCl_2(Urea)_2^+ + 2AlCl_4^-$

1.29 V *vs.* (B) (33)

Similar to the reaction mechanism in the IL, symmetrical breaking to $AlCl(Urea)S_4$ is more favorable than asymmetrical products. Given the linear correlation between the scales from two standard electrodes and the same set of $AlCl_2S_x^-$ intermediates, the steps for conversion to shorter polysulfides are expected to be the same.

$AlCl_2S_8^- + 2Al_2Cl_5(Urea)_2^+ + 2e^- = AlCl(Urea)S_7 + AlCl(Urea)S + AlCl_2(Urea)_2^+ + 2AlCl_4^-$

1.47 V *vs.* (B) (34)

$AlCl_2S_8^- + 3/2Al_2Cl_5(Urea)_2^+ + ½\ Al_2Cl_7^- + 2e^- = AlCl_2S_6^- + AlCl(Urea)S_2 + AlCl_2(Urea)_2^+ + 2AlCl_4^-$

1.29 V *vs.* (B) (35)

$AlCl_2S_8^- + Al_2Cl_5(Urea)_2^+ + Al_2Cl_7^- + 2e^- = AlCl_2S_6^- + AlCl_2S_2^- + AlCl_2(Urea)_2^+ + 2AlCl_4^-$

1.23 V *vs.* (B) (36)

$AlCl_2S_8^- + 3/2Al_2Cl_5(Urea)_2^+ + ½\ Al_2Cl_7^- + 2e^- = AlCl_2S_5^- + AlCl(Urea)S_3 + AlCl_2(Urea)_2^+ + 2AlCl_4^-$

1.38 V *vs.* (B) (37)

$AlCl_2S_8^- + 2Al_2Cl_5(Urea)_2^+ + 2e^- = AlCl(Urea)S_5 + AlCl(Urea)S_3 + AlCl_2(Urea)_2^+ + 2AlCl_4^-$

1.41 V *vs.* (B) (38)

$AlCl_2S_8^- + 2Al_2Cl_5(Urea)_2^+ + 2e^- = 2AlCl(Urea)S_4 + AlCl_2(Urea)_2^+ + 2AlCl_4^-$

1.52 V *vs.* (B) **(39)**

$AlCl_2S_8^- + 3/2Al_2Cl_5(Urea)_2^+ + ½\ Al_2Cl_7^- + 2e^- = AlCl_2S_4^- + AlCl(Urea)S_4 + AlCl_2(Urea)_2^+ + 2AlCl_4^-$

1.48 V *vs.* (B) (40)

$AlCl_2S_8^- + Al_2Cl_5(Urea)_2^+ + Al_2Cl_7^- + 2e^- = 2AlCl_2S_4^- + AlCl_2(Urea)_2^+ + 2AlCl_4^-$

1.44 V *vs.* (B) (41)

Preferentially formed $AlCl(Urea)S_4$ can be further oxidized with the transfer of two more electrons.

$AlCl(Urea)S_4 + Al_2Cl_5(Urea)_2^+ + Al_2Cl_7^- + 2e^- = AlCl(Urea)S_3 + AlCl(Urea)S + 1/2AlCl_2(Urea)_2^+ + 5/2AlCl_4^-$

1.22 V *vs.* (B) (42)

$AlCl(Urea)S_4 + Al_2Cl_5(Urea)_2^+ + Al_2Cl_7^- + 2e^- = AlCl_2S_3^- + AlCl(Urea)S + AlCl_2(Urea)_2^+ + 2AlCl_4^-$

1.17 V *vs.* (B) (43)

$AlCl(Urea)S_4 + Al_2Cl_5(Urea)_2^+ + Al_2Cl_7^- + 2e^- = 2AlCl(Urea)S_2 + 1/2AlCl_2(Urea)_2^+ + 5/2AlCl_4^-$

0.90 V *vs.* (B) (44)

$AlCl(Urea)S_4 + Al_2Cl_5(Urea)_2^+ + Al_2Cl_7^- + 2e^- = 2AlCl_2S_2^- + 3/2AlCl_2(Urea)_2^+ + 3/2AlCl_4^-$

0.82 V *vs.* (B) (45)

Further splitting of the S-S bond leads to the smallest polysulfide species

$AlCl(Urea)S_3 + Al_2Cl_5(Urea)_2^+ + Al_2Cl_7^- + 2e^- = AlCl(Urea)S_2 + AlCl(Urea)S + 1/2AlCl_2(Urea)_2^+ + 5/2AlCl_4^-$

1.24 V *vs.* (B) (46)

$AlCl(Urea)S_3 + Al_2Cl_5(Urea)_2^+ + Al_2Cl_7^- + 2e^- = AlCl_2S_2^- + AlCl(Urea)S + AlCl_2(Urea)_2^+ + 2AlCl_4^-$

1.20 V *vs.* (B) (47)

Finally, Al_2S_3 is formed by a reaction step that is identical to that followed in EMImCl ILs.

$AlCl(Urea)S_2 + AlCl(Urea)S + Al_2Cl_5(Urea)_2^+ + 3\ Al_2Cl_7^- + 2e^- = Al_2S_3 + 2\ AlCl_2(Urea)_2^+ + 6\ AlCl_4^-$

0.63 V *vs.* (B) (48)

Following the same type of analysis described in the previous section, the discharge potentials for these reaction steps (reaction no. 33, 39, 42, 46, 48) are 1.29, 1.52, 1.22, 1.24, 0.63 V, respectively. We predict the observable main discharge plateau at 0.63 V at a discharge current rate low enough (i.e., in the absence of kinetic overpotentials), and the charging plateau at 1.52 V. In short, both the charge and discharge plateaus are lowered (compared to the reaction network with IL participation), but the total charge-discharge hysteresis loss remains the same at around 0.9 V.

3.3. Comparison to experiments

In this section, we compare the predictions of the ab-initio calculations of the electrochemical behavior of Al-S cells and the spectroscopic signatures of polysulfide reaction intermediates with previously reported experimental data, when available.

3.3.1. Charge/discharge behavior of Al-S cells

For Al/S batteries with EMImCl-based electrolytes, discharge plateaus of 0.5 V[15], 0.65 V[24], 0.75 V[14], 0.95 V[25], 1.2 V[8] have been reported. When Urea-based IL is used (or acetamide-based IL with very similar chemistry), the discharge potential falls to 0.4 V[10] (0.55 V[9] and 0.4 V[10] for acetamide-based IL). Our evaluation of discharge potential follows the same trend of decreasing from 0.83 V for traditional ILs (where cations are not electrochemically active) to 0.63 V for Urea-based IL (where the cations facilitate the formation of reaction intermediates). The charging plateau for EMImCl and similar electrolytes has been measured at 1.5 V[10,14] 1.4 V[24] 1.25 V[15]. Our charging potential is estimated to be 1.43 V and is in agreement with these published experimental results for EMImCl or similar ILs. The charging plateau evaluated by us for Urea-based IL at 1.52 V is also close to a value of 1.65 V recently reported[10].

3.3.2. Spectroscopy of reaction intermediates

Our reaction mechanism analysis leads to reaction intermediates that might be characterized with spectroscopy, e.g., $AlCl_2S_8^-$, $AlCl_2S_4^-$, $AlCl(Urea)S_8$ and $AlCl(Urea)S_4$. Here we report UV-vis, IR, and Raman spectra of these species and compare them to published experimental results. We should remark that, in general, the accuracy of computational prediction of UV-vis signatures is limited.

Cohn et al. reported UV-vis spectroscopy measurements of the EMImCl-based electrolyte before and after the discharge of Al/S cells, showing that the pure electrolyte had absorption peaks close to 250 nm, 300 nm and 360 nm, and after discharge, the peak at higher wavenumbers disappeared while the peak at around 300 nm rose in intensity.[8] Similar UV-vis spectra, with very broad peaks, have been reported for discharged sulfur electrodes from Al-S cells in EMImCl-based electrolyte[14,25]. Our calculaitons of polysulfide species indeed predict a large number of UV vis bands with low intensity, with the intensity decreasing with increasing wavenumbers, in agreement with the previously reported experimental results. The calculation of the UV-vis spectra of different polysulfide species also show that it would be difficult to identify the nature of polysulfide species with only UV-vis data.The calculated IR and Raman spectra show bigger differences between the polysulfide species, and therefore, seem a more promising method of the identification of Al-S battery reaction intermediates.

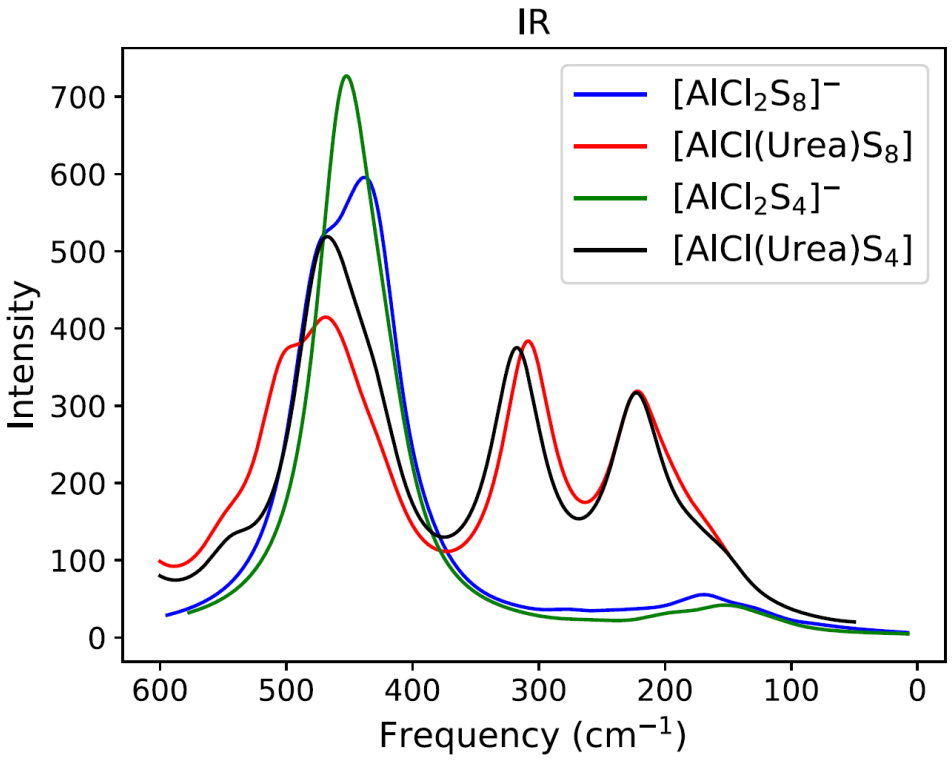

(a)

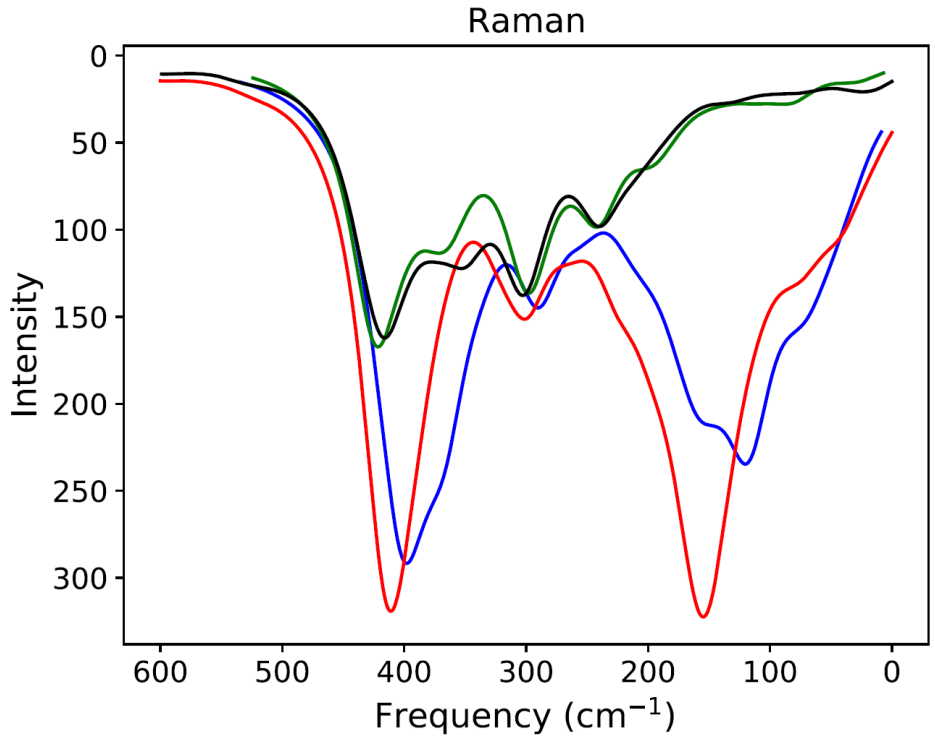

(b)

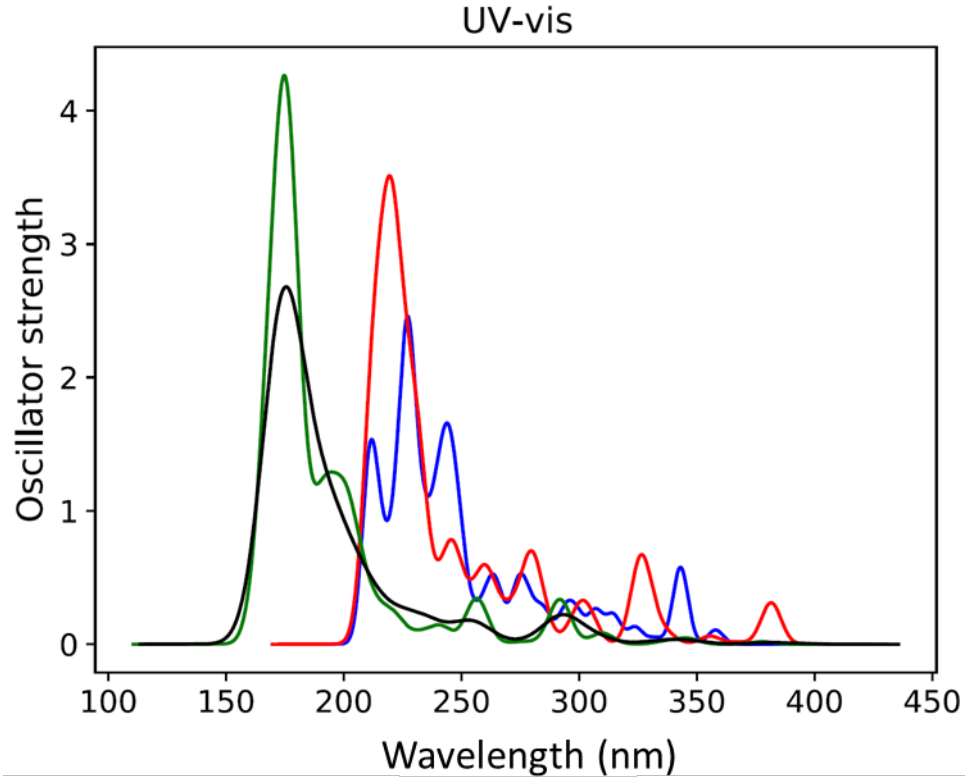

(c)

Figure 3: Computed (a)IR (b) Raman and (c) UV-vis apectra for $AlCl_2S_8^-$, $AlCl(Urea)S_8$, $AlCl_2S_4^-$ and $AlCl(Urea)S_4$. Intensities and oscillator strength have arbitrary units.

4. Conclusion

Using computational methods, we have studied the electrochemical reaction pathway of the discharge and charge reaction Al/S batteries with two types of IL electrolytes: the conventional EMImCl-based IL and DES

electrolytes like urea/$AlCl_3$. The most likely reaction pathway has been identified by computing the Gibbs free energies of the different possible reaction steps, and the potential values referred to the aluminium electrode potential scale, which then give the voltage values of the Al/S batteries.

We demonstrate that an accurate prediction of the discharge and charge behavior of Al/S batteries requires to take into account the strong interaction of polysulfide species with aluminium ions. In particular, we show that the most stable polysulfide species are of the form of complexes such as $AlCl_2S_x^-$ and $AlCl(Urea)S_x$, while isolated S_x^{2-} polysulfides do the exist in an Al/S battery environment.

We find that the discharge reaction of the sulfur electrode initiates with the ring opening of the S_8 molecule, which breaks into smaller polysulfide fragments that are coordinated to aluminium ions that, in turn, are coordinated to choride and, for the deep eutectic solvent, urea ligands. To further characterize the reaction intermediates and mechanisms presented here, we have calculated IR, Raman, and UV-vis spectra of four important reaction intermediates: $AlCl_2S_x^-$ and $AlCl(Urea)S_x$ (x=8,4). In addition, the predictions of the discharge and charge voltages of Al/S cells (0.83 / 1.43 V and 0.63 / 1.52 V for traditional and Urea-based IL, respectively) matches satisfactorily to the range of measured potentials reported in the literature.

We believe that the detailed molecular understanding obtained in this work will be very useful for further developments of Al/S batteries, and we also hope that this work will inspire further experimental work to investigate the spectroscopic signatures of the proposed reaction intermediates here reported.

Acknowledgements

The authors acknowledge the financial support for this work from the European Commission through the Horizon 2020 FET-OPEN project SALBAGE (Grant agreement ID: 766581). We also thank all members of the SALBAGE project for fruitful scientific discussions. NGA thanks the EPSRC for an early career fellowship (EP/N024303/1).

References

(1) Dunn, B.; Kamath, H.; Tarascon, J.-M. Electrical Energy Storage for the Grid: A Battery of Choices. *Science* **2011**, *334* (6058), 928–935. https://doi.org/10.1126/science.1212741.

(2) Elia, G. A.; Marquardt, K.; Hoeppner, K.; Fantini, S.; Lin, R.; Knipping, E.; Peters, W.; Drillet, J.-F.; Passerini, S.; Hahn, R. An Overview and Future Perspectives of Aluminum Batteries. *Advanced Materials* **2016**, *28* (35), 7564–7579. https://doi.org/10.1002/adma.201601357.

(3) Hong, X.; Mei, J.; Wen, L.; Tong, Y.; Vasileff, A. J.; Wang, L.; Liang, J.; Sun, Z.; Dou, S. X. Nonlithium Metal–Sulfur Batteries: Steps Toward a Leap. *Advanced Materials* **2019**, *31* (5), 1802822. https://doi.org/10.1002/adma.201802822.

(4) Chung, S.-H.; Manthiram, A. Current Status and Future Prospects of Metal–Sulfur Batteries. *Advanced Materials* **2019**, *31* (27), 1901125. https://doi.org/10.1002/adma.201901125.

(5) Mamantov, G.; Hvistendahl, J. Rechargeable High Voltage Low Temperature Molten, Salt Cell Na/β''-Alumina/SCl3+ in AlCl3-NaCl. *Journal of Electroanalytical Chemistry and Interfacial Electrochemistry* **1984**, *168* (1), 451–466. https://doi.org/10.1016/0368-1874(84)87115-4.

(6) Marassi, R.; Laher, T. M.; Trimble, D. S.; Mamantov, G. Electrochemical and Spectroscopic Studies of Sulfur in Aluminum Chloride-N-(N-Butyl)Pyridinium Chloride. *J. Electrochem. Soc.* **1985**, *132* (7), 1639. https://doi.org/10.1149/1.2114180.

(7) Peramunage, D.; Licht, S. A Solid Sulfur Cathode for Aqueous Batteries. *Science* **1993**, *261* (5124), 1029–1032. https://doi.org/10.1126/science.261.5124.1029.

(8) Cohn, G.; Ma, L.; Archer, L. A. A Novel Non-Aqueous Aluminum Sulfur Battery. *Journal of Power Sources* **2015**, *283*, 416–422. https://doi.org/10.1016/j.jpowsour.2015.02.131.

(9) Chu, W.; Zhang, X.; Wang, J.; Zhao, S.; Liu, S.; Yu, H. A Low-Cost Deep Eutectic Solvent Electrolyte for Rechargeable Aluminum-Sulfur Battery. *Energy Storage Materials* **2019**, *22*, 418–423. https://doi.org/10.1016/j.ensm.2019.01.025.

(10) Lampkin, J.; Li, H.; Furness, L.; Raccichini, R.; Garcia-Araez, N. A Critical Evaluation of the Effect of Electrode Thickness and Side Reactions on Electrolytes for Aluminum–Sulfur Batteries. *ChemSusChem* **2020**, *13* (13), 3514–3523. https://doi.org/10.1002/cssc.202000447.

(11) Carrasco-Busturia, D.; Lysgaard, S.; Jankowski, P.; Vegge, T.; Bhowmik, A.; García-Lastra, J. M. Ab Initio Molecular Dynamics Investigations of the Speciation and Reactivity of Deep Eutectic

Electrolytes in Aluminum Batteries. *ChemSusChem* **2021**, *14* (9), 2034–2041. https://doi.org/10.1002/cssc.202100163.
(12) Bhauriyal, P.; Das, S.; Pathak, B. Theoretical Insights into the Charge and Discharge Processes in Aluminum–Sulfur Batteries. *J. Phys. Chem. C* **2020**, *124* (21), 11317–11324. https://doi.org/10.1021/acs.jpcc.0c01358.
(13) Wu, S.-C.; Ai, Y.; Chen, Y.-Z.; Wang, K.; Yang, T.-Y.; Liao, H.-J.; Su, T.-Y.; Tang, S.-Y.; Chen, C.-W.; Wu, D. C.; Wang, Y.-C.; Manikandan, A.; Shih, Y.-C.; Lee, L.; Chueh, Y.-L. High-Performance Rechargeable Aluminum–Selenium Battery with a New Deep Eutectic Solvent Electrolyte: Thiourea-AlCl3. *ACS Appl. Mater. Interfaces* **2020**, *12* (24), 27064–27073. https://doi.org/10.1021/acsami.0c03882.
(14) Yu, X.; Boyer, M. J.; Hwang, G. S.; Manthiram, A. Room-Temperature Aluminum-Sulfur Batteries with a Lithium-Ion-Mediated Ionic Liquid Electrolyte. *Chem* **2018**, *4* (3), 586–598. https://doi.org/10.1016/j.chempr.2017.12.029.
(15) Yang, H.; Yin, L.; Liang, J.; Sun, Z.; Wang, Y.; Li, H.; He, K.; Ma, L.; Peng, Z.; Qiu, S.; Sun, C.; Cheng, H.-M.; Li, F. An Aluminum–Sulfur Battery with a Fast Kinetic Response. *Angewandte Chemie International Edition* **2018**, *57* (7), 1898–1902. https://doi.org/10.1002/anie.201711328.
(16) Bian, Y.; Li, Y.; Yu, Z.; Chen, H.; Du, K.; Qiu, C.; Zhang, G.; Lv, Z.; Lin, M.-C. Using an AlCl3/Urea Ionic Liquid Analog Electrolyte for Improving the Lifetime of Aluminum-Sulfur Batteries. *ChemElectroChem* **2018**, *5* (23), 3607–3611. https://doi.org/10.1002/celc.201801198.
(17) Miguel, Á.; Jankowski, P.; Pablos, J. L.; Corrales, T.; López-Cudero, A.; Bhowmik, A.; Carrasco-Busturia, D.; Ellis, G.; García, N.; García-Lastra, J. M.; Tiemblo, P. Polymers for Aluminium Secondary Batteries: Solubility, Ionogel Formation and Chloroaluminate Speciation. *Polymer* **2021**, *224*, 123707. https://doi.org/10.1016/j.polymer.2021.123707.
(18) Li, H.; Lampkin, J.; Garcia-Araez, N. Facilitating Charge Reactions in Al-S Batteries with Redox Mediators. *ChemSusChem* **2021**, *14* (15), 3139–3146. https://doi.org/10.1002/cssc.202100973.
(19) Lin, Z.; Mao, M.; Yang, C.; Tong, Y.; Li, Q.; Yue, J.; Yang, G.; Zhang, Q.; Hong, L.; Yu, X.; Gu, L.; Hu, Y.-S.; Li, H.; Huang, X.; Suo, L.; Chen, L. Amorphous Anion-Rich Titanium Polysulfides for Aluminum-Ion Batteries. *Science Advances 7* (35), eabg6314. https://doi.org/10.1126/sciadv.abg6314.
(20) Sun, H.; Wang, W.; Yu, Z.; Yuan, Y.; Wang, S.; Jiao, S. A New Aluminium-Ion Battery with High Voltage, High Safety and Low Cost. *Chem. Commun.* **2015**, *51* (59), 11892–11895. https://doi.org/10.1039/C5CC00542F.
(21) Kravchyk, K. V.; Kovalenko, M. V. Aluminum Electrolytes for Al Dual-Ion Batteries. *Commun Chem* **2020**, *3* (1), 1–9. https://doi.org/10.1038/s42004-020-00365-2.
(22) Tsuda, T. Aluminum and Zinc Metal Anode Batteries. In *Next Generation Batteries: Realization of High Energy Density Rechargeable Batteries*; Kanamura, K., Ed.; Springer: Singapore, 2021; pp 565–580. https://doi.org/10.1007/978-981-33-6668-8_49.
(23) Tu, J.; Song, W.-L.; Lei, H.; Yu, Z.; Chen, L.-L.; Wang, M.; Jiao, S. Nonaqueous Rechargeable Aluminum Batteries: Progresses, Challenges, and Perspectives. *Chem. Rev.* **2021**, *121* (8), 4903–4961. https://doi.org/10.1021/acs.chemrev.0c01257.
(24) Gao, T.; Li, X.; Wang, X.; Hu, J.; Han, F.; Fan, X.; Suo, L.; Pearse, A. J.; Lee, S. B.; Rubloff, G. W.; Gaskell, K. J.; Noked, M.; Wang, C. A Rechargeable Al/S Battery with an Ionic-Liquid Electrolyte. *Angewandte Chemie International Edition* **2016**, *55* (34), 9898–9901. https://doi.org/10.1002/anie.201603531.
(25) Yu, X.; Manthiram, A. Electrochemical Energy Storage with a Reversible Nonaqueous Room-Temperature Aluminum–Sulfur Chemistry. *Advanced Energy Materials* **2017**, *7* (18), 1700561. https://doi.org/10.1002/aenm.201700561.
(26) Miguel, Á.; Fornari, R. P.; García, N.; Bhowmik, A.; Carrasco-Busturia, D.; García-Lastra, J. M.; Tiemblo, P. Understanding the Molecular Structure of the Elastic and Thermoreversible AlCl3 : Urea/Polyethylene Oxide Gel Electrolyte. *ChemSusChem* **2020**, *13* (20), 5523–5530. https://doi.org/10.1002/cssc.202001557.
(27) Fuoss, R. M. Review of the Theory of Electrolytic Conductance. *J Solution Chem* **1978**, *7* (10), 771–782. https://doi.org/10.1007/BF00643581.
(28) Velde, G. te; Bickelhaupt, F. M.; Baerends, E. J.; Guerra, C. F.; Gisbergen, S. J. A. van; Snijders, J. G.; Ziegler, T. Chemistry with ADF. *Journal of Computational Chemistry* **2001**, *22* (9), 931–967. https://doi.org/10.1002/jcc.1056.
(29) Stephens, P. J.; Devlin, F. J.; Chabalowski, C. F.; Frisch, M. J. Ab Initio Calculation of Vibrational Absorption and Circular Dichroism Spectra Using Density Functional Force Fields. *J. Phys. Chem.* **1994**, *98* (45), 11623–11627. https://doi.org/10.1021/j100096a001.

(30) Grimme, S.; Ehrlich, S.; Goerigk, L. Effect of the Damping Function in Dispersion Corrected Density Functional Theory. *Journal of Computational Chemistry* **2011**, *32* (7), 1456–1465. https://doi.org/10.1002/jcc.21759.
(31) Vijayakumar, M.; Govind, N.; Walter, E.; D. Burton, S.; Shukla, A.; Devaraj, A.; Xiao, J.; Liu, J.; Wang, C.; Karim, A.; Thevuthasan, S. Molecular Structure and Stability of Dissolved Lithium Polysulfide Species. *Physical Chemistry Chemical Physics* **2014**, *16* (22), 10923–10932. https://doi.org/10.1039/C4CP00889H.
(32) Klamt, A.; Schüürmann, G. COSMO: A New Approach to Dielectric Screening in Solvents with Explicit Expressions for the Screening Energy and Its Gradient. *Journal of the Chemical Society, Perkin Transactions 2* **1993**, *0* (5), 799–805. https://doi.org/10.1039/P29930000799.
(33) Wakai, C.; Oleinikova, A.; Ott, M.; Weingärtner, H. How Polar Are Ionic Liquids? Determination of the Static Dielectric Constant of an Imidazolium-Based Ionic Liquid by Microwave Dielectric Spectroscopy. *J. Phys. Chem. B* **2005**, *109* (36), 17028–17030. https://doi.org/10.1021/jp053946+.
(34) Gaudoin, R.; Foulkes, W. M. C.; Rajagopal, G. Ab Initiocalculations of the Cohesive Energy and the Bulk Modulus of Aluminium. *J. Phys.: Condens. Matter* **2002**, *14* (38), 8787–8793. https://doi.org/10.1088/0953-8984/14/38/303.
(35) OQMD http://oqmd.org/ (accessed 2021 -05 -22).
(36) Nørskov, J. K.; Rossmeisl, J.; Logadottir, A.; Lindqvist, L.; Kitchin, J. R.; Bligaard, T.; Jónsson, H. Origin of the Overpotential for Oxygen Reduction at a Fuel-Cell Cathode. *J. Phys. Chem. B* **2004**, *108* (46), 17886–17892. https://doi.org/10.1021/jp047349j.
(37) Abood, H. M. A.; Abbott, A. P.; Ballantyne, A. D.; Ryder, K. S. Do All Ionic Liquids Need Organic Cations? Characterisation of [AlCl2·nAmide]+AlCl4− and Comparison with Imidazolium Based Systems. *Chem. Commun.* **2011**, *47* (12), 3523–3525. https://doi.org/10.1039/C0CC04989A.
(38) Wang, L.; Zhang, T.; Yang, S.; Cheng, F.; Liang, J.; Chen, J. A Quantum-Chemical Study on the Discharge Reaction Mechanism of Lithium-Sulfur Batteries. *Journal of Energy Chemistry* **2013**, *22* (1), 72–77. https://doi.org/10.1016/S2095-4956(13)60009-1.
(39) Angell, M.; Zhu, G.; Lin, M.-C.; Rong, Y.; Dai, H. Ionic Liquid Analogs of AlCl3 with Urea Derivatives as Electrolytes for Aluminum Batteries. *Advanced Functional Materials* **2020**, *30* (4), 1901928. https://doi.org/10.1002/adfm.201901928.

TOC graphics